Hindawi
Journal of Nanomaterials
Volume 2022, Article ID 3203057, 10 pages
https://doi.org/10.1155/2022/3203057

Research Article

Wear Behavior and FESEM Analysis of LM 25 Alloy MMHCs Reinforced with FE_3O_4 and Gr by Utilizing Taguchi's Technique

G. Gokilakrishnan,[1] R. Sathishkumar,[2] N. S. Sivakumar,[3] S. Kaliappan,[4] S. Sekar,[5] Pravin P. Patil,[6] Ram Subbiah,[7] K. P. Yuvaraj,[8] and Feleke Worku Tadesse[9]

[1]*Department of Mechanical Engineering, Sri Eshwar College of Engineering, Coimbatore, Tamil Nadu, India*
[2]*Department of Electrical and Electronics Engineering, SRM TRP Engineering College, Trichy, Tamil Nadu, India*
[3]*Mechatronics Engineering, Tishk International University, Erbil, Kurdistan Region, Iraq*
[4]*Department of Mechanical Engineering, Velammal Institute of Technology, Chennai, Tamil Nadu, India*
[5]*Department of Mechanical Engineering, Rajalakshmi Engineering College, Rajalakshmi Nagar Thandalam, Chennai, 602 105 Tamil Nadu, India*
[6]*Department of Mechanical Engineering, Graphic Era Deemed to be University, Bell Road, Clement Town, Dehradun, Uttarakhand, India*
[7]*Department of Mechanical Engineering, Gokaraju Rangaraju Institute of Engineering and Technology, Hyderabad, Telangana, India*
[8]*Department of Mechanical Engineering, Sri Krishna College of Engineering and Technology, Coimbatore, Tamil Nadu, India*
[9]*School of Mechanical and Industrial Engineering, Institute of Technology, Debre Markos University, Debre Markos, Ethiopia*

Correspondence should be addressed to Feleke Worku Tadesse; wwfeleke@gmail.com

Received 22 April 2022; Accepted 21 June 2022; Published 19 July 2022

Academic Editor: V. Vijayan

The current research is concerned with the production of an LM25-FE3O4—Gr metal matrix hybrid composites (MMHCs) and the analysis of its dry sliding wear conditions. The hybrid composites were made out of 3 wt% Fe3O4 and 4 wt% Gr particles with a mesh size of 200 meshes and were made using the stir casting method. Wear test on Taguchi's L9 orthogonal arrays employs three process parameters: load, sliding velocity, and distance, each changed for three levels on a pin-on-disc tester position. The wear behavior of hybrid composite was investigated using loads of 20 N, 40 N, and 60 N; velocities of 2 m/s, 4 m/s, and 6 m/s; and distances of 1,000 m, 2,000 m, and 3,000 m. The major parameters were developed utilizing the signal-to-noise ratio by selecting "smaller-is-better" wear rates and COF features. FESEM was used to look at the worn surfaces of the composite specimen in order to determine the wear mechanism. Wear properties are enhanced in materials having aluminium hybrid metal matrix composites. According to the ANOVA table, the load parameter has the greatest impact on wear resistance and coefficient of friction, with maximum load values of 35.64 N and 5.782 N, respectively.

1. Introduction

The applications in engineering and technology are increasingly using hybrid composite materials. Compared to natural composite materials, they provide a number of benefits including increased mechanical and physical properties [1]. Aluminium alloys are commonly used to manufacture aerospace, defense, medical equipment, and automotive spare parts due to their superior strength-to-weight ratio. With adding suitable amount of metallic or nonmetallic reinforcements and manufactured them as MMCs, the properties of aluminium alloys can be improved. In the aerospace, defense, automobile, marine, medical instruments, and other mechanical industries, MMCs are increasingly being used to replace traditional metallic alloys. To meet the recent demands of advanced engineering applications, researchers have looked into aluminium alloy-based MMCs [2]. Electrical, food, chemical, and marine applications are just a few of

the many applications for the LM25. It is widely used in the automotive industry, where it is commonly used to cast cylinder blocks, wheels, heads, and other parts [3].

AMCs reinforced with iron oxide (Fe_3O_4) were recently developed utilizing a simple and inexpensive industrialized method [4, 5]. This composite's excellent physical and mechanical properties make it an exceptional multipurposeful, lightweight, and proficient material for engineering and technology intentions. This research is required to improve the composite's electrical conductivity due to the effect of Fe_3O_4 [6].

The hardness of the AMCs reinforced with Gr particles decreased with a linear increase in the Gr content, regardless of the manufacturing process used to create the composite materials [7–10]. Because the structure of a bony lubricating film by Gr particles barred straight contact of sliding surfaces and abridged ploughing effects of Al fragment, the wear resistance of AMCs toughened with Gr particles was superior to that of pure aluminium matrix, resulting in easier machining of these composite materials pretend by a variety of techniques [11–14].

With 5% wt of graphite reinforcement, composite compression strength increased by around 108 percent. With 15% graphite reinforcement in the copper matrix, however, there was a significant reduction in compression strength. The wear properties of composite materials have been improved by incorporating graphite into the copper matrix [15]. Suresh et al. manufactured LM25-B4C-Gr-Fe3O4-based hybrid composites by stir casting route and mechanical behaviors. The consequences explained that LM25-B4C-Gr-Fe3O4 hybrid composites must be investigated as an outstanding material wherever high strength, ultimate tensile strength, and wear resistance are enhanced [16, 17]. Radhika et al. calculated mechanical properties and wear characteristics of LM25/SiC/Al2O3 hybrid MMCs and fabricated by utilized liquid metallurgy route. The results of worn out surfaces of composites were investigated using SEM and it was found that the mechanical properties and wear resistance augmented as the weight percentage of reinforcement augmented [18]. Siddesh Matti et al. synthesized and evaluated the wear behavior Al7075 alloy composites reinforced with mica, fly ash, and red mud particles prepared by stir casting route. The findings of the hybrid composites were subjected to microstructural studies and wear properties testing is improved [19].

Nagarajan Lenin et al. investigated manufacturing and machining of LM25 reinforced with fly ash and boron carbide (B4C) hybrid composites by using stir casting and WEDM. The results showed the composite's mechanical and machining properties are improved and to be used in several engineering applications [20]. Radhika and Raghu developed LM25/TiC MMCs using liquid metallurgy process and the mechanical properties such as hardness and tensile strength were enhanced on the composite. The microstructural assessment divulges that uniform spreading was achieved in the composites [21]. Gowthamkumar et al. modelled the influence of solidification and flow rate of the molten alloy in a recycled aluminium LM-25 alloy with a high Fe concentration. Mechanical and microstructural characterizations were used to assess the flow ability and mechanical behavior of cast aluminium scrap, which was compared to a FEA model through simulation [22]. Squeeze casting was used to study and investigate the sliding wear behavior of LM 25, Al/10 wt. percent fly ash composites, AA/10 wt. percent steel particles composites, and AA/5wt. percent FA/5 wt. percent SP hybrid composites. However, Al/FA/SP hybrid composites outperformed Al alloy, Al/FA, and Al/SP composites in terms of wear resistance [23]. Hiremath investigated LM25-borosilicate glass particle composites using the stir casting method, and the findings show that the hardness improves linearly as the reinforcement amount inside the matrix increases. It is also clear that the cold material's Volumetric Heat Capacities have a significant impact not only on the quality of the castings produced but also on the hardness of the AMCs [24]. Elango et al. [11] studied the wear properties of LM25 and composites supplemented with SiC and Titanium Dioxide (TiO2). The strengthening enhanced the wear resistance of the LM 25 alloy, according to the findings [25].

Table 1: Chemical composition of LM25 aluminium alloy.

Composition	%
Si	7.23
Fe	0.73
Cu	0.12
Mn	0.14
Mg	0.29
Cr	0.02
Ni	0.02
Sn	0.01
Ti	0.02
Pb	0.01
Zn	0.14
Al	Balance

Figure 1: Casted LM25-FE_3O_4-Gr MMHCs specimen.

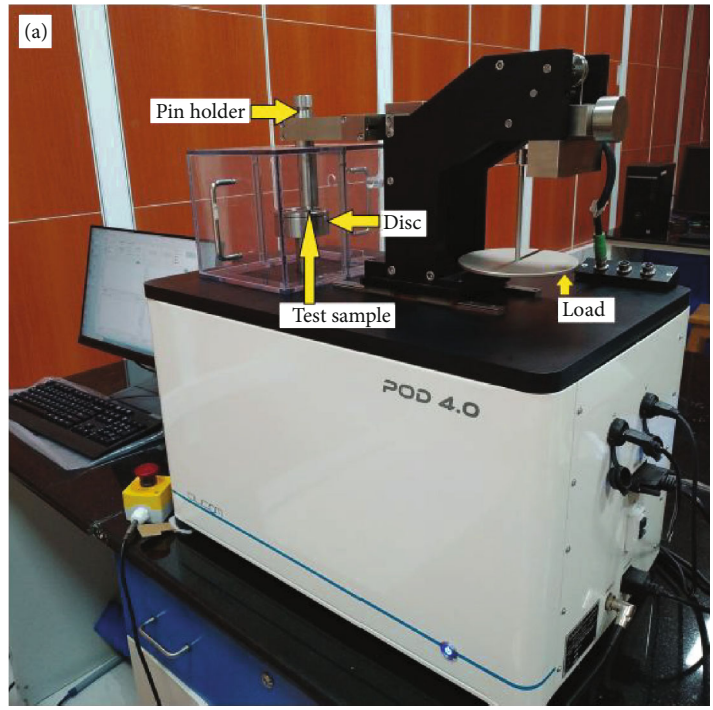

Figure 2: Wear testing machine.

In Technology and Science, the signal-to-noise ratio (SNR) is defined as a calculation that compares the level of a chosen signal to the level of background noise [26]. In this case, SNR is calculated by comparing the signal inside a material's imperfection region to the signal within the material's sound area. The SNR is defined as the ratio of the signal intensity recorded in the ROI, i.e., the inhomogeneous area of the specimen, to the standard deviation of the signal intensity in an area outside the ROI [26].

The SNR can be calculated in a variety of methods, according to scientific literature. A list of seven commonly used SNR equations in the scientific community is shown below [27].

$$\text{SNR} = \frac{\text{ALS}}{\text{SD}} \quad (1)$$

where

SNR = signal-to-noise ratio

ALS= the average level of the signal in the defect region

SD= the standard deviation of the noise in the reference or sound region

According to the literature, LM25 aluminium alloy hybrid metal matrix composite reinforced with 3 wt% Fe3O4 and 4 wt% Gr particles was produced by stir casting route to improve the wear properties for automotive, aerospace, and industrial tenders. The tribological behavior of the composite is still being investigated using Taguchi's method to estimate the wear rate and coefficient of friction.

Table 2: Process parameters and their levels.

Levels	Load (N)	Sliding velocity (m/s)	Sliding distance (m)
1	20	2	1000
2	40	4	2000
3	60	6	3000

2. Materials and Methods

2.1. Material Selection. The LM25 aluminium alloy, with a density of 2.68 gm/cm^3 and properties such as weight, toughness, and temperature transfer, was chosen as the base medium due to its use in automotive pistons. The reinforcement of Fe_3O_4 particles with 200 mesh sizes was chosen to improve wear resistance. It has a density of 5.24 gm/cm^3, a superior hardness than SiC, WC, and TiC, and exceptional substance and thermal permanence, making it an ideal reinforcement for improving the alloy's wear performance. The graphite, which has a density of 2.26 g/cm^3, is also used as a reinforcement material, and the composite hardness diminishes as the adding percent of graphite (Gr) augments [28, 29]. The substance compositions of the LM25 aluminium alloy were determined using spectroscopy, as shown in Table 1.

2.2. Stir Casting Method. Owing to its outlay—value, the stir casting method was used to manufacture and fabricate the composite. The LM25 major matrix was liquefied in a stir casting setup furnace, encased in a crucible. The alloy was dissolved in a static gas ambiance, which barred substance reactions and resulted in a casting. The preheated

Table 3: L9 orthogonal array.

S.No	Process parameters Load (N)	Velocity (m/s)	Distance (m)	Wear rate (mm^3/m)	S/N ratio (db)	COF	S/N ratio (db)
1	20	2	1000	0.017	35.38	0.527	5.56
2	20	4	2000	0.016	35.71	0.513	5.79
3	20	6	3000	0.016	35.82	0.502	5.98
4	40	2	1000	0.051	25.99	0.583	4.68
5	40	4	2000	0.049	26.04	0.564	4.97
6	40	6	3000	0.047	26.44	0.573	4.83
7	60	2	1000	0.098	20.11	0.543	5.30
8	60	4	2000	0.096	20.31	0.532	5.48
9	60	6	3000	0.093	20.61	0.521	5.66

reinforcements were added during the usual intermission behind liquefy and stirred for 8 minutes at 450 rpm to ensure uniform reinforcement particle distribution. The liquefied metal was then poured into preheated (400°C) moulds with dimensions of 100 x 14 mm and allowed to solidify at 840°C, as shown in Figure 1.

2.3. Wear Test. Figure 2 shows the results of wear tests using a pin-on-disc apparatus provided by DUCOM on a variety of work pieces.

The cast component was turned in a circular specimen with dimensions of 12 mm x 30 mm. The sample was subjected to dry sliding wear tests using a DUCOM pin-on-disc apparatus in accordance with L9 orthogonal arrays [30]. A rotating steel disc (EN-31) with a hardness of VH114 held test pins (12-30 mm) in place. Throughout the experiment, an 80 mm path diameter was maintained. The cantilever beam, which imparts an equivalent amount of energy to the sample that will come into contact with the opposing visage, remained loaded.

The pin is forced into contact with the disc by the applied load. As a result of surface wear, the pin's size adjusts slightly, allowing the lever arm to be transferred. The LVDT measures the separate wear by disarticulating the switch limb. Before and after the experiment, the specimen was dressed appropriately. The sample's mass loss was taken into account and rehabilitated as volume thrashing and, as a result, wear rates.

During standard intermissions, friction sensors were used to calculate the CoF between the pin and the revolving disc, which was then confirmed using the WINDUCOM software. The average coefficient of friction is stretched by taking the average of those values.

2.4. Taguchi's Method. The L9 orthogonal array and Taguchi's method were chosen to achieve the best results with the fewest trials possible, and the experimentation plan remained unchanged (Table 2). The S/N ratio and ANOVA were used to calculate the wear rates of the specimen and the average CoF by using Mini Tab software. The experiment was guided by the following parameters: applied load, sliding velocity, and sliding distance, all of which differed between levels (Table 2).

Table 4: Response table for S/N ratios–wear rate.

Level	Load (N)	Speed (m/s)	Distance (m)
1	35.64	27.16	27.16
2	26.16	20.69	20.69
3	13.68	27.63	27.63
Delta	21.96	6.94	6.94
Rank	1	2	3

Table 5: Response means–wear rate.

Level	Load (N)	Speed (m/s)	Distance (m)
1	0.006918	0.007063	0.007783
2	0.009143	0.007167	0.008070
3	0.005987	0.007817	0.006203
Delta	0.002187	0.001650	0.001870
Rank	1	2	3

2.5. Field Emission Scanning Electron Microscopy (FESEM). In the microanalysis and failure analysis of solid inorganic materials, field emission scanning electron microscopy (FESEM) is widely used. High exaggerations, high-resolution imagery, and precise measurements of very small facial features and objects are all possible with scanning electron microscopy. FESEM presents absolute elevated declaration descriptions of the sample by focusing an electron beam transversely across the surface.

3. Results and Discussion

3.1. Tribological Behavior. The composite's tribological behavior was assessed, including wear rates and coefficients of friction. The results and their S/N ratios are shown in Table 3. The investigation's findings were assessed using ANOVA, which is used to investigate the stimulus of the considered wear strictures, namely, applied load, sliding

Table 6: ANOVA result.

Sources	Degree of freedom (DF)	Squares sum (seq SS)	Mean square (adj MS)	F value	P value	Contribute level (%)	Error (%)
Load (N)	2	12.191	6.575	0.88	0.641	35.46	2.8
Speed (m/s)	2	7.391	4.196	0.56	0.577	29.63	1.5
Distance (m)	2	8.356	4.628	0.63	0.743	25.85	1.7

speed, and sliding distance, all of which have a significant impact on routine measures. Using analysis of variance, it is possible to determine unambiguously which independent variable rules over the others, as well as the percentage contribution of those independent variables.

For the aluminium alloy LM25, 4% Gr, and 3% Fe_3O_4, the ANOVA results for wear rate and COF for three factors varied at three levels and interfaces for three levels and interfaces. The lower value of wear rates is 0.00355 at a velocity of 6 m/s and a load of 20 N. The higher value of wear rates is 0.01367 at a velocity of 2 m/s and a load of 60 N.

Table 3 shows that as the composites' velocity augmented, the wear rates of the composites decreased. The significance level for this analysis is =0.05, which corresponds to a 95 percent confidence level. Sources contributing to the performance measures with a P-value of less than 0.05 were considered statistically significant contributors.

3.2. Analysis of Signal-to-Noise Ratio. Taguchi's technique uses an S/N ratio to specify the position of structure based on their stimulus. Tables 4–6 show S/N ratios of wear rates. For this study, "smaller-is-better" characteristics were used. The delta value of conforming structure is determined by the variation among the peak values. The plunging mandate of the delta value retained its assigned position. In terms of wear rate, load remained the primary constraint, with distance and velocity as its stimuli. The conforming ranking of structure is specified in the last row of Tables 4–6. Finest wear behavior was observed at third levels of load (1st rank) and speed (2nd rank) and 2nd level in sliding distance (3rd rank).

The influence of each parameter on ANOVA results has been calculated, and the load is a major contributing factor that influenced wear performance by 35.46 percent; the next significant parameter is speed percentage, which influenced wear performance by 29.63 percent; and sliding speed, which influenced wear rate by 25.85 percent (Table 6).

The stimulus on the coefficient of friction was ranked first by distance, followed by load and sliding velocity (Tables 7–9). It is possible that the distance rank is due to the presence of tough reinforcements. As the distance between the sliding surfaces grows, the reinforcement particles that protrude from the surface become fissured, aggregating the contact area between the sliding surfaces and reducing friction. The best CoF was found at the third levels of load (1st rank), speed (2nd rank), and sliding distance (2nd level) (3rd rank).

The load is a major contributing factor that influenced wear performance by about 5.86 percent; the next significant parameter is speed percentage, which influenced wear performance by about 4.975 percent; and sliding speed is the last influencing factor that influenced CoF by about 3.569 percent (Table 9).

Table 7: Response table for S/N ratios–coefficient of friction.

Level	Load (N)	Speed (m/s)	Distance (m)
1	5.782	5.185	5.185
2	4.833	5.418	5.418
3	5.483	5.495	5.495
Delta	0.950	0.311	0.311
Rank	1	2	3

Table 8: Response means–CoF.

Level	Load (N)	Speed (m/s)	Distance (m)
1	0.005842	0.008496	0.006584
2	0.008456	0.006892	0.007965
3	0.006852	0.009512	0.005431
Delta	0.003258	0.002478	0.002974
Rank	1	2	3

3.3. Influence of Wear Rate Parameters on the Responses. The effects of process variables on wear rates and friction coefficient were studied. As a mean plot, Figure 2(a) depicts the trend of the corresponding responses. Figure 2(b) shows the optimal level of parameters using S/N ratios. The following sections go over the effects of parameters on responses in detail.

3.3.1. Effect of Load. Wear rates increase as the applied load increases, as shown in Figures 3(a) and 3(b). The fringe surge of wear rate remained pragmatic from 20 N to 40 N, whereas the severe surge from 40 N to 60 N was severe. The material's elastic distortion is to blame for this drift. Temperature increases to the sliding surface had fewer effects on the elastic distortion at low loads (20 N and 40 N). Adding a load (60 N) to the specimen causes a temperature spike over the sliding surface, even at slow sliding velocities. The high temperature caused plastic deformation of the surface, resulting in the adhesion of pin surfaces to the disc. As a result of this adhesion, more material is removed, dramatically increasing wear rates [31].

3.3.2. Effect of Distance. Wear rates were found to be decreasing as distance increased. The converse kin is construed by this diminishing to drift, as shown in Figures 2(a) and 2(b). When comparing the wear rate between 1,000 m and 2,000 m to the wear rate between

Table 9: ANOVA result.

Sources	Degree of freedom (DF)	Squares sum (seq SS)	Mean square (adj MS)	F value	P value	Contribute level (%)	Error (%)
Load (N)	2	10.782	5.658	0.75	0.598	5.86	2.5
Speed (m/s)	2	6.235	3.259	0.61	0.657	4.975	1.6
Distance (m)	2	9.456	4.980	0.54	0.862	3.569	1.4

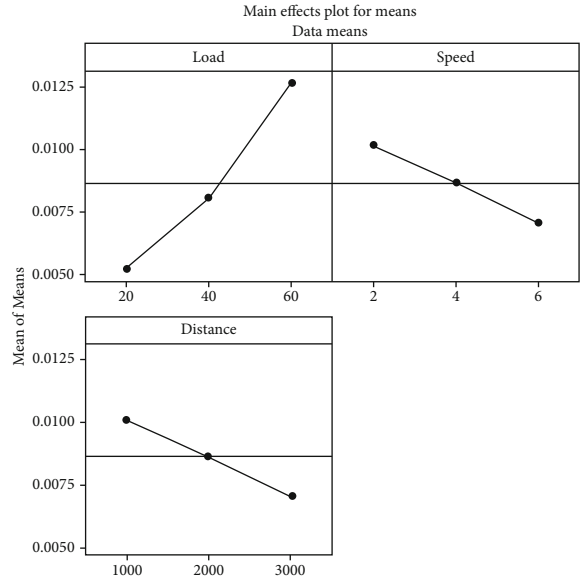

(a)

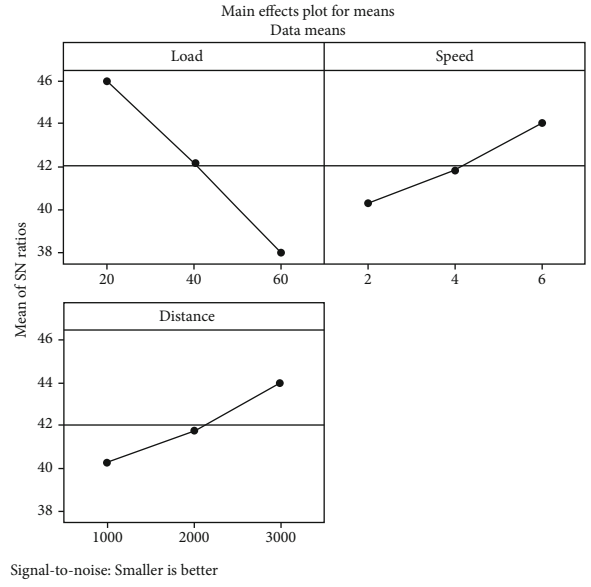

(b)

Figure 3: (a) Main effect plot for means–wear rate. (b) Main effect plot for S/N ratios–wear rate.

2,000 m and 3,000 m, the wear rate between 1,000 m and 2,000 m decreased significantly. The behavior be capable of stabilized through the incidence of stiff reinforcements that appear as piercing brusqueness on the composite specimen's surface. Reinforcement particles that protrude from the composite surface reduce the area among the specimen and the disc at first, which augments the wear rate and CoF.

The distance among the sliding surfaces increases; these asperities become compacted and blunt, escalating the area among the sliding surfaces [32]. This possibly explains the improved wear behavior at long distances.

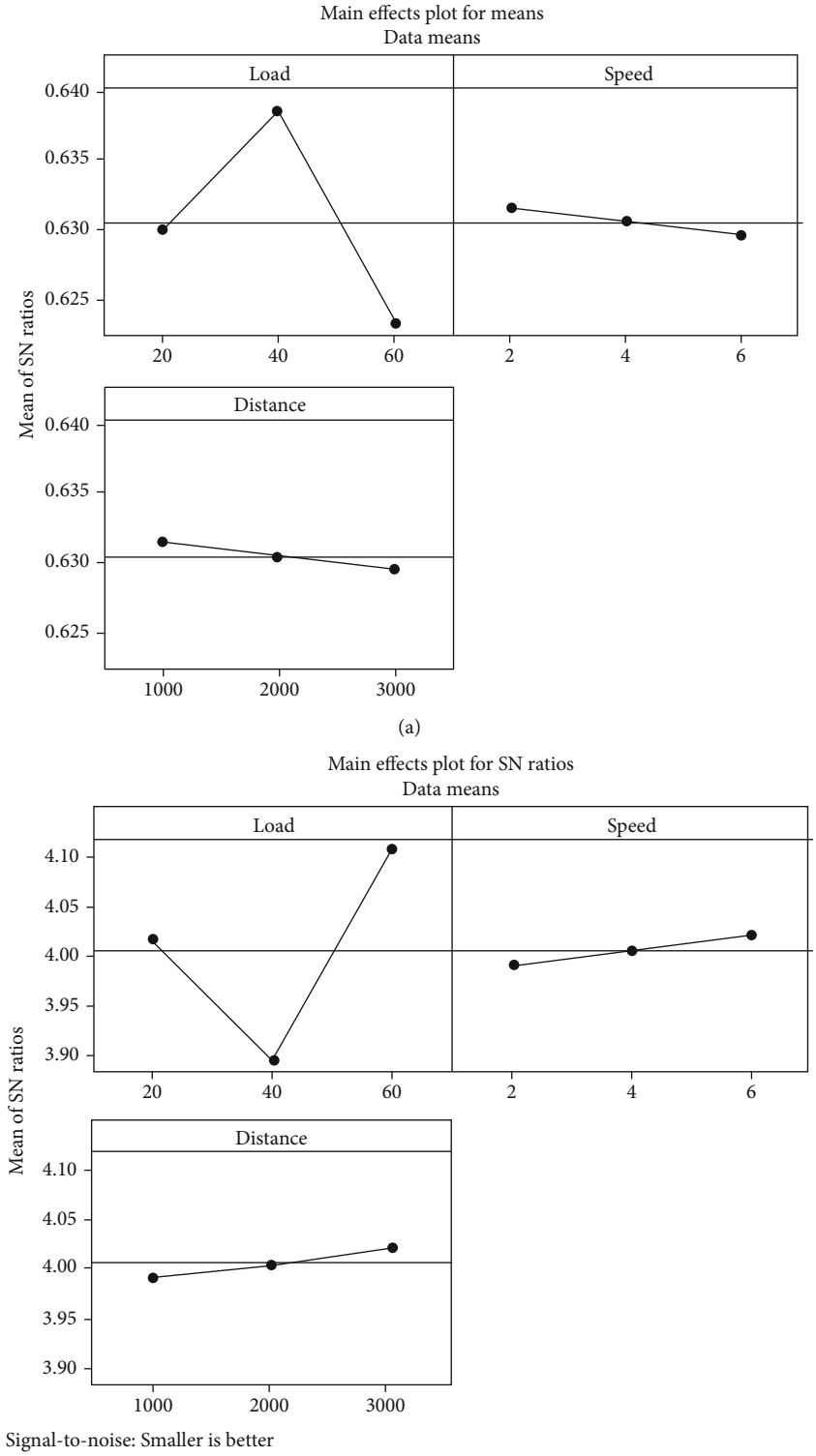

Figure 4: (a) Main effect plot for means–coefficient of friction. (b) Main effect plot for S/N ratios–coefficient of friction.

3.3.3. Effect of Velocity. With increasing velocity, the rejoinders were pragmatic to be diminishing (Figures 2(a) and 2(b)). The formation of a tribo-layer can help with this. The aluminium has the ability to form an oxide layer on its external fringe. The temperature of the contact surface rises when sliding at high speeds, causing the material to corrode. This miracle refers to the transport of materials in the form of a mechanically mixed layer, also known as a tribo-layer. This film determination acted as a barricade or lubricant among the surfaces during velocity upsurges,

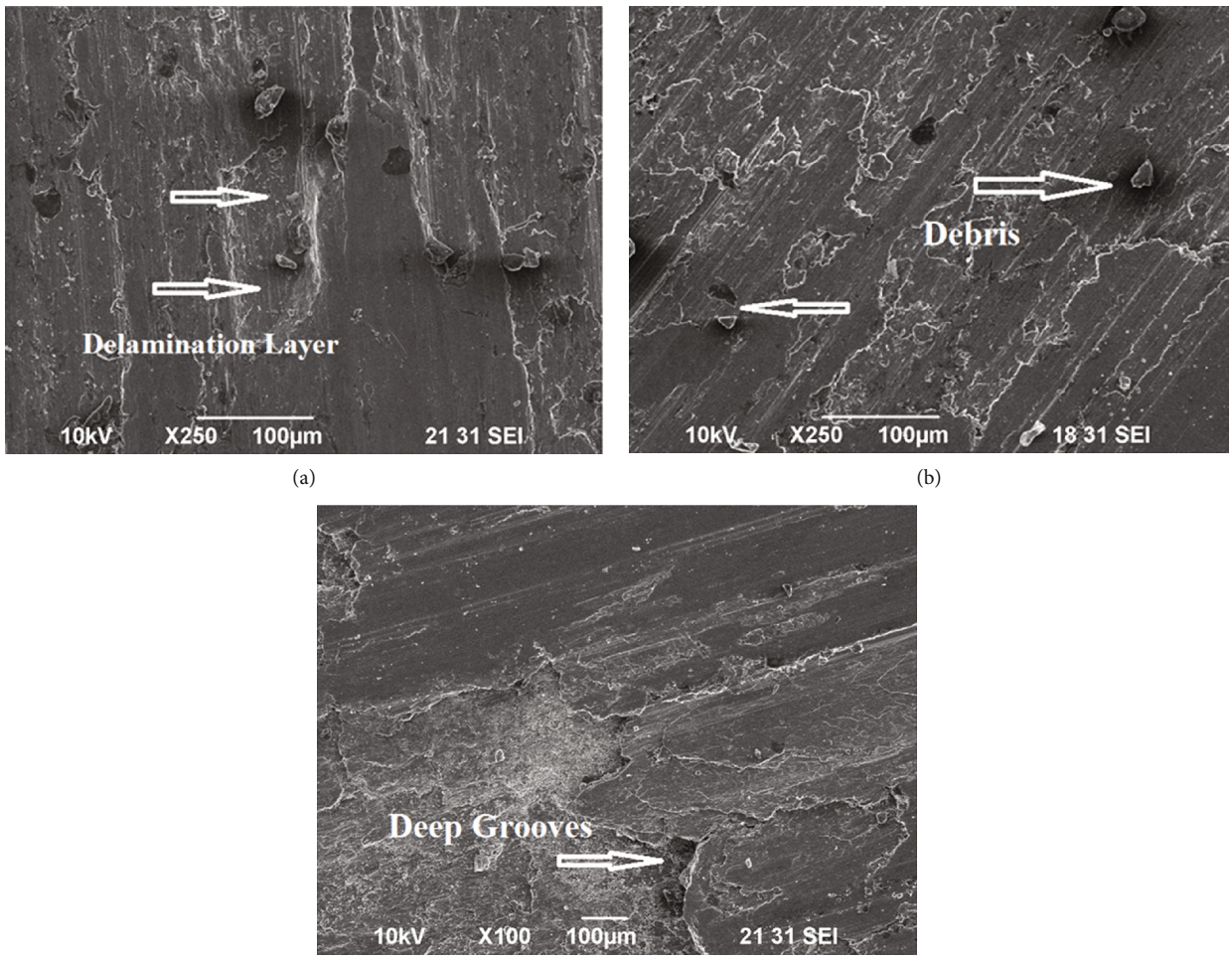

Figure 5: (a–c) Typical SEM micrographs of composites.

reducing wear rates [33]. The stumpy load (20 N), superior sliding velocity (6 m/s), and greatest distance were the best parameters for improving the composite's tribological behavior (3,000 m).

3.4. Influence of Coefficient of Friction Parameters on the Responses. The consequence of progression strictures on the CoF was still being assessed. Figure 4(a) depicts the drift of the agreeing reply angrily, while Figure 4(b) depicts the finer echelon of strictures utilizing S/N ratios. The effects of strictures on reply angrily were conversed in depth in the progressive segments.

3.4.1. Effect of Load. The coefficient of friction increases as the applied load increases, as shown in Figures 3(a) and 3(b). The fragmentation of the oxide layer can cause an increase in coefficient of friction. At stumpy loads, the particles that were hauling lacking throughout downhill react among the impression and structure of the film. The temperature over the contact surface had a big impact on this boron oxide film. The friction among the sliding surfaces is increased as a result [34].

3.4.2. Effect of Distance. As the distance between the two points grows, the CoF appears to be diminishing. The converse kin is construed by reducing to drift, as shown in Figures 4(a) and 4(b). When comparing the CoF between 1,000 m and 2,000 m to the COF between 2,000 m and 3,000 m, the CoF between 1,000 m and 2,000 m decreased significantly. The occurrence of stiff reinforcements that proceed as piercing brusqueness on the surface of the composite specimen can brace the behavior.

3.4.3. Effect of Velocity. As the velocity augments, these film acts as an obstruction or lubricant among the surfaces, diminishing the CoF (Figures 4(a) and 4(b)).

3.5. FESEM Analysis. The use of a FESEM to examine wear surfaces fashioned into dry sliding wear in a stable environment is an important tool for determining composite wear and tear behavior. Figure 5 shows composites with morphological decorations such as cavernous permanent undulations, micro pits, debris, and broken particles on their wear surfaces. The dilapidated façade of the Al-Fe3O4-Gr composite (Figure 5(a)) shows the presence of delaminated layers. The sliding surface depicted in this diagram has been

clearly stimulated by the stratum. The surfaces appear smooth as well, thanks to the graphite reinforcement. On the surface of the Al- Fe3O4-Gr composite, deep grooves can be seen (Figure 5(b)), which may have contributed to the increased wear loss.

The surface of the Al-Fe3O4-Gr composite (Figure 5(c)) clearly reveals fragments and kaput particles. Imprecise dances and fine scuff had formed on the worn surface. The wear mechanisms are defined by the structure of undulations, which are shaped by the humanizing exploit of stiff abruptness on the counteract disc and toughened dilapidated fragments. If the amount of boron carbide was increased, wear would be reduced. At high speeds, the temperature rises faster than the sliding surface, causing the material to oxidize and the material to transfer between the pin and counter face, resulting in the formation of MML. This layer contributes to good tribological properties at high speeds [35–37].

4. Conclusions

The following explanation was faded commencing this present investigative work:

(i) The stir casting route was used to successfully fabricate an LM25 aluminium alloy hybrid metal matrix composite reinforced with 3 wt% Fe_3O_4 and 4 wt% Gr particles

(ii) The wear rate and CoF have an unswerving relationship among the load, but are inversely related to the sliding speed and distance, according to tribological findings

(iii) The wear and tear rate was determined primarily by load, pursued by distance and sliding velocity, whereas the CoF is influenced disproportionately by distance, pursued by load and sliding velocity

(iv) Stumpy load (20 N), superior sliding velocity (6 m/s), and most distance were the best circumstances for attaining superior tribological characteristics (3,000 m).

(v) At high velocities, SEM analysis exposed the wear mechanism. This research into tribological behavior can be put to good use in determining the supreme materials for use in the automotive industry, wherever sliding contact is predictable

(vi) For a longer component life, conformist automotive elements such as pistons, piston liners, brake rotors, and cylinder heads can be replaced among these AMCs

Data Availability

The data used to support the findings of this study are included in the article. Should further data or information be required, these are available from the corresponding author and upon request.

Conflicts of Interest

The authors declare that they have no conflicts of interest.

References

[1] N. Bouhfid, M. Raji, R. Boujmal et al., *Numerical modeling of hybrid composite materials*, Series in Composites Science and Engineering, Woodhead Publishing, 2019.

[2] R. Pandiyarajan, P. Maran, S. Marimuthu, and K. C. Ganesh, "Mechanical and tribological behavior of the metal matrix composite AA6061/ZrO2/C," *Journal of Mechanical Science and Technology*, vol. 31, no. 10, pp. 4711–4717, 2017.

[3] A. Mazahery and M. O. Shabani, "Influence of the hard coated B_4C particulates on wear resistance of Al-Cu alloys," *Composites: Part B*, vol. 43, no. 3, pp. 1302–1308, 2012.

[4] E. Bayraktar and D. Katundi, "Development of a new aluminium matrix composite reinforced with iron oxide (FE3O4)," *Journal Of Achievements In Materials And Manufacturing Engineering*, vol. 38, no. 1, pp. 7–14, 2010.

[5] D. Katundi, F. Ayari, E. Bayraktar, M.-J. Tan, and A. Tosun Bayraktar, "Design of aluminum matrix composites reinforced with nano iron oxide (FE3O4)," in *In: AMPT, 15th international conference on "Advanced materials processing technologies"*no. 2012, pp. 1–12, Australia, 2012.

[6] E. Bayraktar, M.-H. Robert, I. Miskioglu, and A. Tosun Bayraktar, "Mechanical and tribological performance of aluminium matrix composite reinforced with nano iron oxide (FE3O4)," in *Composite, Hybrid, and Multifunctional Materials*, Conference Proceedings of the Society for Experimental Mechanics, G. Tandon, Ed., pp. 185–192, Springer, Cham, 2014.

[7] A. M. Hassan, G. M. Tashtoush, and A. K. J. Ahmed, "Effect of graphite and/or silicon carbide particles addition on the hardness and surface roughness of Al-4 wt% Mg alloy," *Journal of Composite Materials*, vol. 41, no. 4, pp. 453–465, 2007.

[8] F. Akhlaghi and Z. A. Bidaki, "Influence of graphite content on the dry sliding and oil impregnated sliding wear behavior of Al 2024–graphite composites produced by in situ powder metallurgy method," *Wear*, vol. 266, no. 1-2, pp. 37–45, 2009.

[9] A. Baradeswaran and A. E. Perumal, "Wear and mechanical characteristics of Al 7075/graphite composites," *Composites: Part B*, vol. 56, pp. 472–476, 2014.

[10] S. N. Prashant, N. Madeva, and V. Auradi, "Preparation and Evaluation of Mechanical and Wear Properties of 6061Al Reinforced with Graphite Particulate Metal Matrix Composite," *Int. J. Metall. Mater. Sci. Eng*, vol. 2, no. 3, pp. 85–95, 2012.

[11] Y. B. Liu, J. D. Hu, Z. Y. Cao, and P. K. Rohatgi, "Wear resistance of laser processed Al–Si–graphitep composites," *Wear*, vol. 206, no. 1-2, pp. 83–86, 1997.

[12] C. B. Lin, R. J. Chang, and W. P. Weng, "A study on process and tribological behavior of Al alloy/Gr. (p) composite," *Wear*, vol. 217, no. 2, pp. 167–174, 1998.

[13] L. Krishnamurthy, B. K. Sridhara, and B. D. Abdul, "Comparative study on the machinability aspects of aluminium silicon carbide and aluminium graphite composites," *Materials and Manufacturing Processes*, vol. 22, no. 7-8, pp. 903–908, 2007.

[14] V. Suresh, A. D. Praneet, and J. Anoop, "Ingenious analysis on machining parameters of aluminium alloy (LM25)/graphite (Gr)/boron carbide (B4C) hybrid composites using wire electrical discharge machining (WEDM)," *Materials Today Proceedings*, vol. 37, no. 2, pp. 3112–3117, 2021.

[15] J. Kumar and S. Mondal, "Microstructure and properties of graphite-reinforced copper matrix composites," *Journal of the Brazilian Society of Mechanical Sciences and Engineering*, vol. 40, no. 4, p. 196, 2018.

[16] S. Vellingiri, "An experimental and investigation on the microstructure hardness and tensile properties of Al-GrFe3O4 hybrid metal matrix composites," *FME Transactions*, vol. 47, no. 3, pp. 511–517, 2019.

[17] V. Suresh, P. Vikram, R. Palanivel, and R. F. Laubscher, "Mechanical and wear behavior of LM25 Aluminium matrix hybrid composite reinforced with Boron carbide, Graphite and Iron oxide," *Materials Today: Proceedings*, vol. 5, pp. 27852–27860, 2018.

[18] N. Radhika, T. V. Balaji, and S. Palaniappan, "Studies on mechanical properties and tribological behaviour of LM25/SiC/Al2O3 composites," *Journal of Engineering Science and Technology*, vol. 10, no. 2, pp. 134–144, 2019.

[19] S. Matti, B. P. Shivakumar, S. Shashidhar, and M. Nagaral, "Dry sliding wear behavior of Mica, Fly Ash and Red Mud particles reinforced Al7075 alloy hybrid metal matrix composites," *Journal of Science and Technology*, vol. 14, no. 4, pp. 310–318, 2021.

[20] N. Lenin, M. Sivakumar, G. Selvakumar et al., "Optimization of process control parameters for WEDM of Al-LM25/Fly Ash/B4C hybrid composites using evolutionary algorithms: a comparative study," *Metals*, vol. 11, no. 7, p. 1105, 2021.

[21] N. Radhika and R. Raghu, "Prediction of mechanical properties and modeling on sliding wear behaviour of LM25/TiC composite using response surface methodology," *Particulate Science and Technology*, vol. 36, no. 1, pp. 104–111, 2018.

[22] K. Gowthamkumar, G. Sathiyaseelan, and C. Bhagyanathan, "Effect of strontium (Sr) and iron (Fe) on solidification process of recycled aluminum LM-25 alloy," *International Research Journal of Engineering and Technology*, vol. 6, no. 6, pp. 2792–2795, 2019.

[23] P. Shanmughasundaram, D. P. Venkatesh, N. Ashok, and N. T. Demeke, "Influence of temperature on tribological behaviour of dual reinforced aluminium MMCs," *Journal Of Mines, Metals & Fuels*, vol. 68, no. 6, pp. 189–195, 2020.

[24] A. Hiremath, A. Amar Murthy, S. V. Pranavathmaja, A. Jajodia, and R. Sreenath, "Effect of end chills, reinforcement content and carburization on the hardness of LM25-borosilicate glass particulate composite," *Journal of Mechanical Engineering and Sciences*, vol. 12, no. 4, pp. 4203–4215, 2018.

[25] G. Elango, B. K. Raghunath, K. Palanikumar, and K. Tamizhmaran, "Sliding wear of LM25 aluminium alloy with 7.5% SiC+2.5% TiO2 and 2.5% SiC+7.5% TiO2 hybrid composites," *Journal of Composite Materials*, vol. 48, no. 18, pp. 2227–2236, 2014.

[26] W. Marijke and Y. Rosseel, "On the definition of signal-to-noise ratio and contrast-to-noise ratio for fMRI data," *PLoS One*, vol. 8, no. 11, article e77089, 2013.

[27] R. Usamentiaga, C. Ibarra-Castanedo, and X. Maldague, "More than fifty shades of grey: quantitative characterization of defects and interpretation using SNR and CNR," *Journal of Nondestructive Evaluation*, vol. 37, no. 2, p. 25, 2018.

[28] P. Ravindran, K. Manisekar, P. Narayanasamy, N. Selvakumar, and R. Narayanasamy, "Application of factorial techniques to study the wear of Al hybrid composites with graphite addition," *Materials and Design*, vol. 39, pp. 42–54, 2012.

[29] M. Nagaral, R. Pavan, P. S. Shilpa, and V. Auradi, "Tensile behavior of B4C particulate reinforced Al2024 alloy metal matrix composites," *FME Transactions*, vol. 45, pp. 93–96, 2017.

[30] P. Vijian and V. P. Arunachalam, "Optimization of squeeze cast parameters of LM6 aluminium alloy for surface roughness using Taguchi method," *Journal of Materials Processing Technology*, vol. 180, no. 1–3, pp. 161–166, 2006.

[31] R. N. Rao and S. Das, "Wear coefficient and reliability of sliding wear test procedure for high strength aluminium alloy and composite," *Materials and Design*, vol. 31, no. 7, pp. 3227–3233, 2010.

[32] L. Zhang, X. B. He, X. H. Qu, B. H. Duan, X. Lu, and M. L. Qin, "Dry sliding wear properties of high volume fraction SiCp/Cu composites produced by pressure less infiltration," *Wear*, vol. 265, no. 11–12, pp. 1848–1856, 2008.

[33] F. Gul and A. Mehmet, "Effect of the reinforcement volume fraction on the dry sliding wear behaviour of Al-10Si/SiCp composites produced by vacuum infiltration technique," *Composite Science and Technology*, vol. 64, no. 13–14, pp. 1959–1966, 2004.

[34] M. Uthayakumar, S. Aravindan, and K. Rajkumar, "Wear performance of Al-SiC-B_4C hybrid composites under dry sliding conditions," *Materials and Design*, vol. 47, p. 456, 2013.

[35] S. Basavarajappa, G. Chandramohan, A. Mahadevan, M. Thangavelu, R. Subramanian, and P. Gopalakrishnan, "Influence of sliding speed on the dry sliding wear behaviour and the subsurface deformation on hybrid metal matrix composite," *Wear*, vol. 262, no. 7–8, pp. 1007–1012, 2007.

[36] V. Suresh, N. Hariharan, S. Paramesh, M. Prasath Kumar, and P. Arun Prasath, "Tribological behaviour of aluminium/boron carbide (B4C)/graphite (Gr) hybrid metal matrix composite under dry sliding motion by using ANOVA," *International Journal of Materials and Product Technology*, vol. 53, no. 3/4, pp. 204–217, 2016.

[37] V. Suresh, N. Hariharan, and S. Vellingiri, "An investigation on the tensile properties and micro-structure of hybrid metal matrix composites," *International Journal of Materials and Product Technology*, vol. 56, no. 1/2, pp. 84–94, 2018.